

CATALYTIC FAST PYROLYSIS OF CELLULOSE MIXED WITH SULFATED TITANIA TO PRODUCE LEVOGLUCOSENONE: ANALYTICAL PY-GC/MS STUDY

Qiang Lu,^{a,*} Xu-Ming Zhang,^a Zhi-Bo Zhang,^a Ying Zhang,^b Xi-Feng Zhu,^b and Chang-Qing Dong^{a,*}

Sulfated titania ($\text{SO}_4^{2-}/\text{TiO}_2$) was prepared and used for catalytic fast pyrolysis of cellulose to produce levoglucosenone (LGO), a valuable anhydrosugar product. Analytical pyrolysis-gas chromatography/mass spectrometry (Py-GC/MS) technique was employed in this study to achieve the catalytic fast pyrolysis of cellulose and on-line analysis of the pyrolysis vapors. Experiments were performed to investigate the effects of several factors on the LGO production, *i.e.* pyrolysis temperature, cellulose/catalyst ratio, TiO_2 crystal type, and pyrolysis time. The results indicated that the $\text{SO}_4^{2-}/\text{TiO}_2$ catalyst lowered the initial cellulose decomposition temperature and altered the pyrolytic product significantly. Levoglucosan (LG) was the most abundant product in the non-catalytic process, while levoglucosenone (LGO) was the major product in the catalytic process. The maximal LGO yield was obtained at the set pyrolysis temperature of 400 °C, while the highest LGO content was obtained at 350 °C, with the peak area% over 50%. In addition, the $\text{SO}_4^{2-}/\text{TiO}_2$ (anatase) was confirmed the best catalyst for the LGO production.

Keywords: Levoglucosenone; Cellulose; Fast pyrolysis; Catalysis; Sulfated titania

Contact information: a: National Engineering Laboratory for Biomass Power Generation Equipment, North China Electric Power University, Beijing 102206, China; b: Key Laboratory for Biomass Clean Energy of Anhui Province, University of Science and Technology of China, Hefei 230026, China;

*Corresponding author: qianglu@mail.ustc.edu.cn, cqdong1@163.com

INTRODUCTION

Fast pyrolysis of biomass to produce bio-oil is one of the most promising technologies to utilize lignocellulosic biomass, and it has received extensive attention in recent years (Bridgwater and Peacocke 2000; Mohan *et al.* 2006). Chemically, bio-oil is a complex mixture containing many valuable chemicals, and thus it has the potential for useful chemicals recovery. However, most of the chemicals in bio-oil are in low contents, making their recovery not only technically difficult, but also economically unattractive at present (Czernik and Bridgwater 2004). To obtain specific value-added chemicals, it is necessary to selectively control the biomass pyrolysis pathways to produce specific bio-oil with high contents of target products, known as the selective fast pyrolysis technique.

Levoglucosenone (LGO, 1,6-anhydro-3,4-dideoxy- β -D-pyranosen-2-one, or 6,8-dioxabicyclo[3.2.1]oct-2-en-4-one) is a sugar enone product of cellulose, formed via the combined depolymerization and dehydration reactions (Halpern *et al.* 1973; Ohnishi *et al.* 1975). It is an optically active organic compound in which all carbon atoms are in different environments and have easily modifiable functional groups. As a result, LGO

can be used in the synthesis of various products, such as tetrodotoxin, thiosugar, and ras activation inhibitors (Shafizadeh *et al.* 1979; Miftakhov *et al.* 1994).

The LGO is usually formed at very low yield during fast pyrolysis of cellulose or biomass, but the yield can be increased in the presence of proper acid catalysts in the pyrolysis process. Various acid catalysts exhibited the capability to promote the LGO formation, such as the MgCl_2 and FeCl_3 (Klampfl *et al.* 2006), $(\text{NH}_4)_2\text{SO}_4$ and $(\text{NH}_4)_2\text{HPO}_4$ (Pappa *et al.* 2006; Di Blasi *et al.* 2007), CrO_3 and $\text{CrO}_3+\text{CuSO}_4$ (Fu *et al.* 2008a), ZnCl_2 (Di Blasi *et al.* 2008; Branca *et al.* 2010; Lu *et al.* 2011a), M/MCM-41 (M=Sn, Zr, Ti, Mg, etc.) (Torri *et al.* 2009), nano TiSiO_4 , and $\text{Al}_2\text{O}_3\cdot\text{TiO}_2$ (Fabbri *et al.* 2007a, b). However, most of these catalysts showed poor catalytic selectivity on the production of LGO, because they would catalyze to increase the yield of several dehydrated products. Until now, only three catalysts have been reported to be promising for LGO production with high selectivity, including the H_3PO_4 (Dobele *et al.* 2001; Dobele *et al.* 2003; Sarotti *et al.* 2007; Fu *et al.* 2008b; Nowakowski *et al.* 2008), $\text{Fe}_2(\text{SO}_4)_3$ (Dobele *et al.* 2005), and H_2SO_4 (Branca *et al.* 2011; Sui *et al.* 2012). To obtain LGO, the cellulose or biomass should be impregnated with these catalysts, and then subjected to fast pyrolysis. During fast pyrolysis process, the presence of one of the three catalysts would significantly promote the depolymerization and dehydration of cellulose to generate the LGO, meanwhile inhibit most of the other competing pyrolytic reactions to obtain the LGO with high selectivity.

Recently, we prepared sulfated metal oxides and used them for catalytic conversion of cellulose fast pyrolysis products. In the first study, pure cellulose was subjected to fast pyrolysis and the pyrolysis vapors were catalytically converted by three sulfated metal oxides (Lu *et al.* 2009). The yield of LGO was increased, but it was not the major product, because this catalytic mode had a greater tendency to promote the formation of three furan derivatives. In the second study, sulfated zirconia ($\text{SO}_4^{2-}/\text{ZrO}_2$) was mechanically mixed with the cellulose, and the mixture was subjected to fast pyrolysis in a lab-scale fixed-bed reactor (Wang *et al.* 2011). In this catalytic mode, the LGO was produced with high selectivity, and the highest yield was over 8% at the pyrolysis temperature as low as 335 °C. The results indicated that sulfated metal oxides could be effective catalysts for LGO production. However, due to the limitation of the experimental set, it is difficult to reveal the detailed formation characteristics of the LGO and other pyrolytic products under different reaction conditions.

Compared with the H_3PO_4 , $\text{Fe}_2(\text{SO}_4)_3$, and H_2SO_4 catalysts, the utilization of solid sulfated metal oxides to produce LGO will offer significant advantages on feedstock pretreatment and catalyst recycles, and thus, deserves further investigation. In this study, two sulfated titania ($\text{SO}_4^{2-}/\text{TiO}_2$) catalysts were prepared using nano anatase TiO_2 and rutile TiO_2 , respectively. They were mechanically mixed with the cellulose and then subjected to fast pyrolysis using the analytical Py-GC/MS technique, which is a powerful tool for primary catalyst selection and evaluation. Experiments were performed to investigate the influence of four parameters on the pyrolytic product distribution, including the pyrolysis temperature, pyrolysis time, cellulose/catalyst ratio, and TiO_2 crystal type.

EXPERIMENTAL

Materials

The feedstock used in this study included commercial microcrystalline cellulose (Avicel PH-101) and pure levoglucosan (LG), purchased from Sigma.

Catalysts Preparation and Characterization

Two sulfated titania ($\text{SO}_4^{2-}/\text{TiO}_2$) catalysts were prepared by using commercial nano-anatase TiO_2 and nano-rutile TiO_2 (purchased from Aladdin). In a typical procedure, 10 g of TiO_2 (anatase or rutile) was impregnated with 1 mol/L aqueous sulfuric acid with stirring for 12 h. Afterwards, the mixture was filtered, dried at 110 °C for 24 h, and finally calcined at 525 °C for 3 h to obtain the $\text{SO}_4^{2-}/\text{TiO}_2$ (anatase) or $\text{SO}_4^{2-}/\text{TiO}_2$ (rutile). The two parent TiO_2 and two $\text{SO}_4^{2-}/\text{TiO}_2$ were used as the catalysts in this study.

The textural properties of the catalysts were analyzed using a ChemBET PULSAR analyzer. The surface area was determined using the Brunauer-Emmett-Teller (BET) method, and the pore volume was determined by the Barrett-Joyner-Halenda (BJH) method. The sulfur content was measured by an Elementar vario MACRO cube analyzer.

X-ray diffraction (XRD) analysis was conducted with a Philips X'pert PRO X-ray diffractometer, which employed Cu $K\alpha$ radiation ($\lambda = 0.15418$ nm). The data were recorded over the 2θ range of 10 to 70°. Crystalline phases were identified by comparison with the reference data from the International Center for Diffraction Data (ICDD) files.

Fourier transform infrared (FTIR) analysis was performed using a Perkin Elmer spectrophotometer. The catalysts were mixed with KBr and the mixtures were pressed into pellets for analysis. The absorption frequency spectra were recorded and plotted at room temperature. The standard IR-spectra were used to identify the functional groups of the catalysts.

Analytical Pyrolysis

The analytical Py-GC/MS experiments were performed using the CDS Pyroprobe 5200HP pyrolyser (Chemical Data Systems) connected with the Perkin Elmer GC/MS (Clarus 560). During the preparation of the experimental samples, the pyrolysis tube was firstly filled with a quartz rod and some tightly pressed quartz wool. Afterwards, 0.30 mg cellulose and a certain amount of catalyst (0.30 mg, 0.60 mg, or 0.90 mg) were filled above the quartz wool and mechanically mixed together. Finally, some quartz wool was placed above the cellulose/catalyst mixture to prevent the escape of solid particles. An analytical balance with the readability of 0.01 mg was used for weighing.

The pyrolysis was carried out at the set temperature from 300 °C to 500 °C and selected times of 5 s, 10 s, and 20 s, respectively. The heating rate was 20 °C/ms. Because of the poor thermal conductivity of cellulose, its actual pyrolysis temperature would be lower than the set value, reported as 50 to 100 °C lower according to the unit's book (Pattiya *et al.* 2008).

The pyrolysis vapors were analyzed by GC/MS. The injector temperature was kept at 300 °C. The chromatographic separation was performed using an Elite-35MS capillary column (30 m \times 0.25 mm i.d., 0.25 μm film thickness). Helium (99.999%) was

used as the carrier gas with a constant flow rate of 1 mL/min at a 1:80 split ratio. The oven temperature was programmed from 40 °C (3 min) to 280 °C with the heating rate of 10 °C/min. The temperature of the GC/MS interface was held at 280 °C, and the mass spectrometer was operated in EI mode at 70 eV. The mass spectra were obtained from m/z 20 to 400. The chromatographic peaks were identified according to the NIST library, Wiley library, and the literature data of previous studies.

For each sample, the experiments were conducted at least three times to confirm the reproducibility of the reported procedures. For each identified product, the average values of the peak area and peak area % were calculated for analysis. In addition, the standard deviation values were also calculated. The Py-GC/MS technique could not provide the direct quantitative analysis of the compounds, due to the complexity of the pyrolytic products and the lack of commercially available standards for them. However, the chromatographic peak area of a compound is considered linear with its quantity, and the peak area % is linear with its content. Therefore, for each product, its average peak area value obtained under different reaction conditions can be compared to reveal the changing of its yields, and the peak area % value can be compared to show the changing of its relative content among the detected products.

RESULTS AND DISCUSSION

Catalyst Properties

The XRD patterns of the two TiO₂ and two SO₄²⁻/TiO₂ catalysts are given in Fig. 1. The two SO₄²⁻/TiO₂ only exhibited typical peaks of the crystalline phases of their parent TiO₂, which suggested that the TiO₂ structure was not altered after the impregnation and calcination process. The properties of the four catalysts are given in Table 1. It is seen that the anatase TiO₂ had higher BET surface area, but smaller particle size and pore volume than the rutile TiO₂. In regard to the two SO₄²⁻/TiO₂ catalysts, both of their BET surface areas and pore volumes were decreased considerably compared to their parent TiO₂. In addition, the SO₄²⁻/TiO₂ (anatase) had larger particle size than the TiO₂ (anatase), while the SO₄²⁻/TiO₂ (rutile) and TiO₂ (rutile) had similar particle sizes.

Table 1. Properties of the Catalysts

Catalyst	BET Surface Area (m ² /g)	Pore Volume (cm ³ /g)	Particle Size (nm)	Sulfur Content (wt. %)
TiO ₂ (anatase)	142.8	0.41	9.8	--
TiO ₂ (rutile)	45.3	0.80	16.2	--
SO ₄ ²⁻ /TiO ₂ (anatase)	62.5	0.24	14.1	3.9
SO ₄ ²⁻ /TiO ₂ (rutile)	26.3	0.25	16.5	4.5

The FTIR spectra of the four catalysts are shown in Fig. 2. In the spectra of the two SO₄²⁻/TiO₂ catalysts, the peaks between 900 cm⁻¹ and 1400 cm⁻¹ were assigned to the stretching vibrations of the S=O bond and the S-O bond, which are characteristic peaks of the sulfated metal oxides. The highest stretching vibration of the SO₄²⁻ in these two

catalysts was above 1200 cm^{-1} , indicating the chelate bidentate SO_4^{2-} coordinated to Ti^{4+} (Guo *et al.* 1994). The strong inductive effect of the S=O bond could make the Ti^{4+} cation a strong acid site.

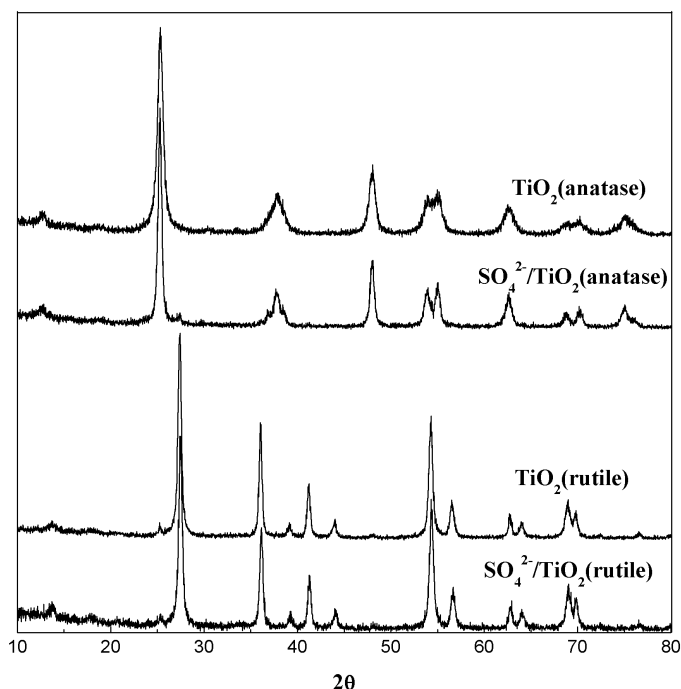


Fig. 1. The XRD patterns of the two TiO_2 and two $\text{SO}_4^{2-}/\text{TiO}_2$ catalysts

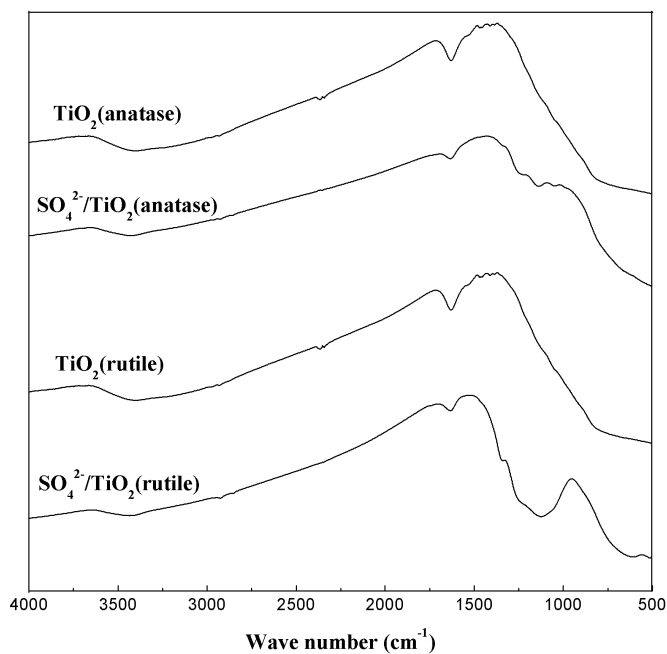


Fig. 2. The FTIR spectra of the two TiO_2 and two $\text{SO}_4^{2-}/\text{TiO}_2$ catalysts

Product Distribution: Cellulose Non-catalytic and Catalytic Fast Pyrolysis

Cellulose fast pyrolysis vapors consist of permanent gases (CO, CO₂, CH₄, H₂, etc.), volatile compounds, and non-volatile oligomers (see Fig. 3).

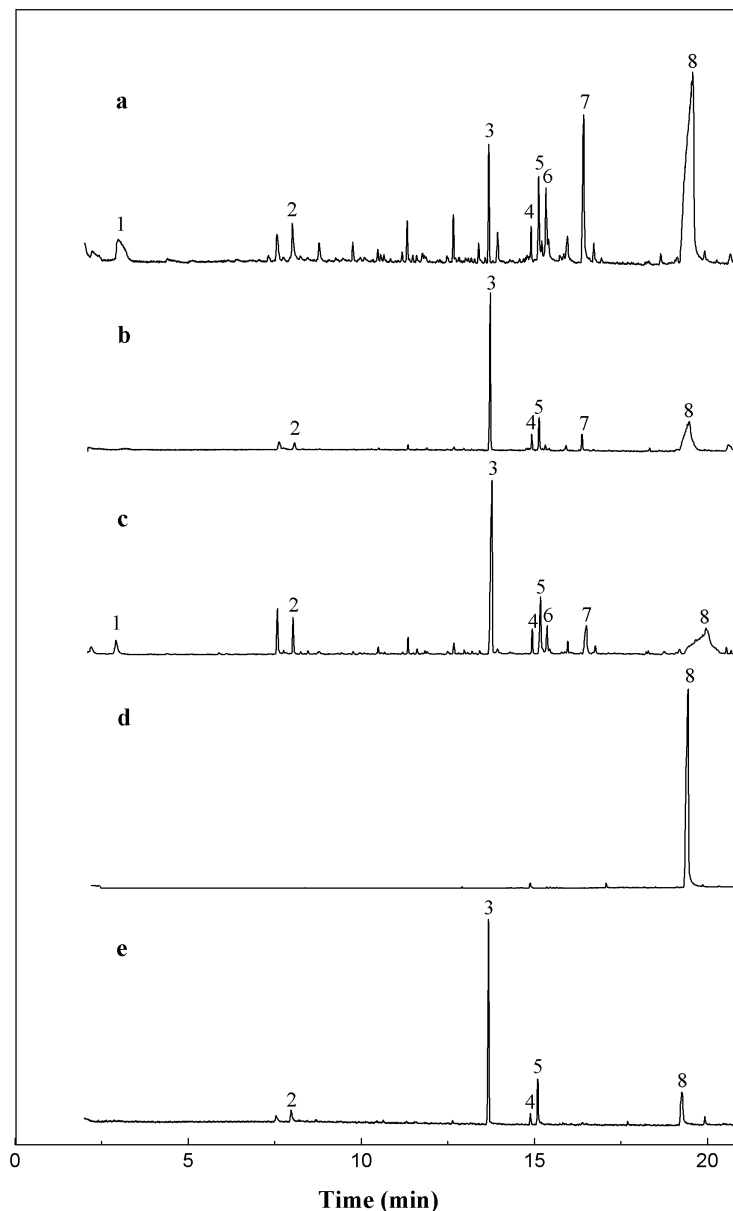


Fig. 3. The typical total ion chromatograms from different pyrolysis conditions.

(a) fast pyrolysis of pure cellulose at 450 °C for 20 s; (b) catalytic pyrolysis of the cellulose at 350 °C for 20 s with the cellulose : SO₄²⁻/TiO₂(anatase) ratio of 1/3; (c) catalytic pyrolysis of the cellulose at 450 °C for 20 s with the cellulose : SO₄²⁻/TiO₂(anatase) ratio of 1/3; (d) fast pyrolysis of pure LG at 400 °C for 20 s; (e) catalytic conversion of the LG at 350 °C for 20 s using the SO₄²⁻/TiO₂(anatase) catalyst

(1) HAA (hydroxyacetaldehyde), (2) FF (furfural), (3) LGO (levoglucosenone), (4) LAC (1-hydroxy-3,6-dioxabicyclo[3.2.1]octan-2-one), (5) DGP (1,4:3,6-dianhydro- α -D-glucopyranose), (6) HMF (5-hydromethyl-furfural), (7) APP (1,5-anhydro-4-deoxy-D-glycero-hex-1-en-3-ulose), (8) LG (levoglucosan)

The condensates of the latter two classes of compounds constitute the liquid bio-oil, while GC/MS was only able to determine the organic volatile compounds. During the non-catalytic fast pyrolysis process, no products were detected by GC/MS when the set pyrolysis temperature was below 400 °C. This indicated that the pure cellulose was not decomposed to form organic volatiles at such low temperatures. At the set temperature of 400 °C and higher, various pyrolytic products were detectable, and the typical total ion chromatogram is shown in Fig. 3(a). The identified pyrolytic products were reported in previous studies (Lu *et al.* 2009; Patwardhan *et al.* 2009; Shen and Gu 2009; Shen *et al.* 2011), and only some important compounds were numbered on the total ion chromatograms. It is seen that the products were mainly the LG, together with some HAA, FF, LGO, LAC, DGP, HMF, and APP. The detailed formation characteristics of these products can be found in our previous study (Lu *et al.* 2011b).

In the catalytic fast pyrolysis process, the pyrolysis behavior and product distribution was changed greatly as compared with the non-catalytic process. First of all, the catalysts lowered the temperature for the initial decomposition of cellulose to form organic volatiles. The pyrolytic products were detectable at the set temperature above 400 °C in the non-catalytic process, but this critical temperature was only 350 °C in the catalytic process. The presence of the catalyst also changed the product distribution greatly, with the typical total ion chromatograms shown in Fig. 3 (b,c). Under the catalysis by the $\text{SO}_4^{2-}/\text{TiO}_2$, the LGO was formed as the major product, together with some FF, DGP, LAC, and APP as important byproducts. The results clearly indicated that the $\text{SO}_4^{2-}/\text{TiO}_2$ catalyst possessed the catalytic capability and selectivity to produce the LGO. Nevertheless, the pure TiO_2 catalyst did not exhibit such catalytic selectivity on the formation of LGO. The detailed distribution of the pyrolytic products under different reaction conditions will be presented and discussed in the following sections.

Effects of Pyrolysis Temperature on the Product Distribution

Pyrolysis temperature played an important role on the product distribution (Fig. 4). Figure 4 gives the peak area and peak area% values of the LG and LGO from non-catalytic and catalytic processes using the TiO_2 (anatase) and $\text{SO}_4^{2-}/\text{TiO}_2$ (anatase) catalysts. The results were obtained at the cellulose/catalyst ratio of 1/2 and pyrolysis time of 20 s.

During the non-catalytic fast pyrolysis of cellulose, the LG was the most abundant product, derived from the sequential cleavage of the two glycosidic bonds on the polysaccharide chain (Ponder *et al.* 1992; Patwardhan *et al.* 2009). On the other hand, the LGO was a minor product, generated from the combined glycosidic bond cleavage and intramolecular dehydration of cellulose (Ohnishi *et al.* 1975). Our previous study reported detailed characteristics of the formation of the two compounds over a wide pyrolysis temperature range. Generally, the formation of the LG was favored at medium temperatures, while the formation of the LGO was favored at low temperatures (Lu *et al.* 2011b). As was shown in Fig. 4, the LG yield (based on its peak area values) was increased greatly from 400 °C to 500 °C, while the maximal LGO yield was obtained at 450 °C.

During the $\text{SO}_4^{2-}/\text{TiO}_2$ -catalyzed fast pyrolysis of cellulose, considerable amounts of products were detected at as low as 350 °C. The relative content of LG (based on the

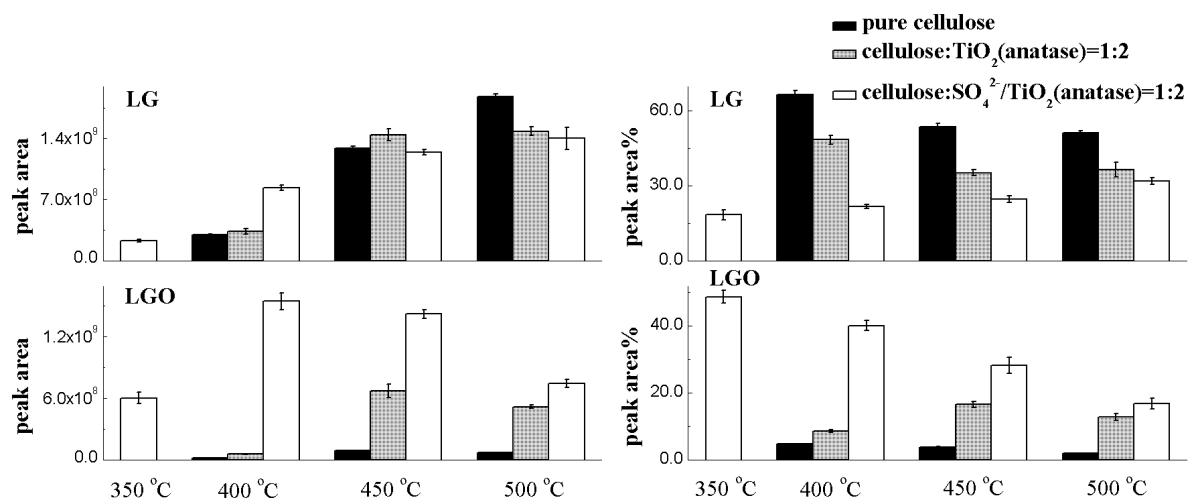


Fig. 4. Peak area and peak area% of the LG and LGO obtained from pure cellulose and cellulose mixed with the TiO₂ (anatase) and SO₄²⁻/TiO₂ (anatase)

peak area% values) was decreased markedly compared to the non-catalytic process. Nevertheless, its yield at 400 °C was higher than that of the non-catalytic process, which should be due to the catalytic effect to lower the decomposition temperature of the cellulose. On the other hand, its yield at 500 °C was lower than those in the non-catalytic process, indicating that the SO₄²⁻/TiO₂ catalyst could inhibit the formation of LG. In this case, both the yield and relative content of LGO increased greatly compared to the non-catalytic process. When the fast pyrolysis temperature was elevated, the LGO yield firstly increased and then decreased, with the maximal yield obtained at 400 °C. As the temperature was raised further, the relative content was decreased monotonically, from 48.7% at 350 °C to 40.1% at 400 °C, 28.2% at 450 °C, and only 16.8% at 500 °C. The results indicated that the catalytic selectivity of the SO₄²⁻/TiO₂ catalyst was high at low temperatures and but would fade at elevated temperatures. Previous studies have also revealed that the formation of the LGO in the acid-catalyzed pyrolysis process was favored at low temperatures (Fabbri *et al.* 2007b). Figure 4 also shows the results from the TiO₂-catalyzed process. The LGO yields were also increased, but in much less degrees than the SO₄²⁻/TiO₂-catalyzed process. This observation suggested that the acidity of the catalyst was very important to the LGO formation.

Besides the LG and LGO, it is necessary to pay attention to other important pyrolytic products; the results are shown in Fig. 5. Among these compounds, the DGP was increased considerably in the catalytic process and became an important by-product. It was generated through the combined intramolecular transglycosylation to form 1,4-anhydride and etherification reaction to form 3,6-anhydride (Shafizadeh *et al.* 1978). Similar as the LGO, the DGP yield was firstly increased and then decreased along with the increasing pyrolysis temperature; the maximal yield was obtained at 450 °C. Its relative content was decreased monotonically, with 7.1% maximal peak area% at 350 °C. In addition, the yields of FF and LAC were also slightly increased in the catalytic process.

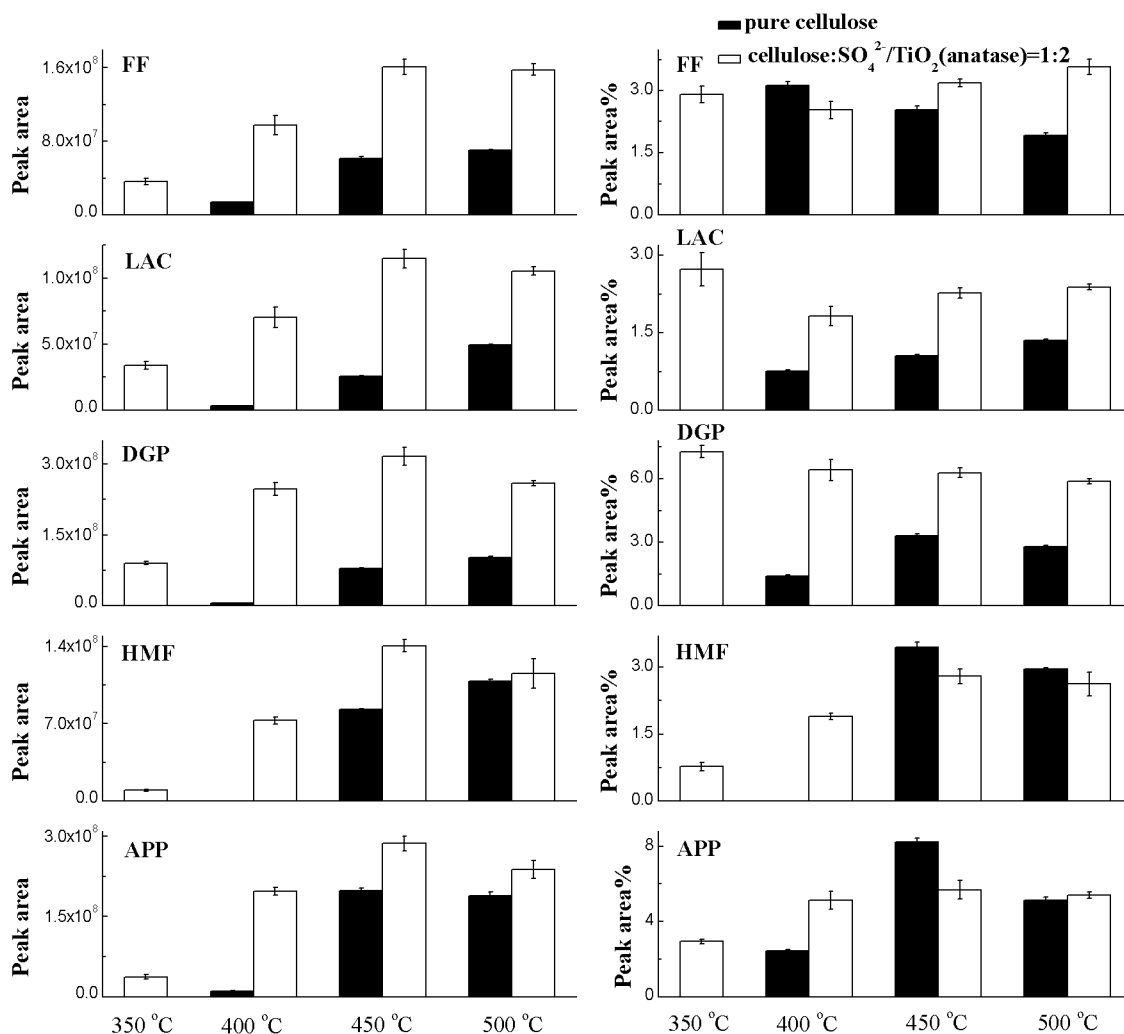


Fig. 5. Peak area and peak area% of the FF, LAC, DGP, HMF and APP obtained from pure cellulose and cellulose mixed with the $\text{SO}_4^{2-}/\text{TiO}_2$ (anatase)

Effects of Cellulose/Catalyst Ratio on the Product Distribution

Cellulose/catalyst ratio was another important factor influencing the pyrolytic product distribution. Figure 6 gives the peak area and peak area% results of the LG and LGO from the non-catalytic and $\text{SO}_4^{2-}/\text{TiO}_2$ (anatase)-catalyzed processes with the cellulose/catalyst ratios of 1/1, 1/2, and 1/3, respectively. The results were obtained at the pyrolysis time of 20 s. The other pyrolytic products as well the results from the TiO_2 (anatase)-catalyzed process are not shown in details here.

As the cellulose/catalyst ratio rising from 1/1 to 1/3, the LGO yield and its relative content were gradually increased. The LG yield was only slightly changed, while its relative content was gradually decreased. The results suggested that the selectivity of $\text{SO}_4^{2-}/\text{TiO}_2$ catalyst on the LGO production would be promoted at elevated catalyst quantity. It was noted that the catalyst quantity used in this study was high, and the catalytic effects were not influenced greatly by the cellulose/catalyst ratio in the studied range. This should be due to the fact that the cellulose/catalyst mixtures were kept

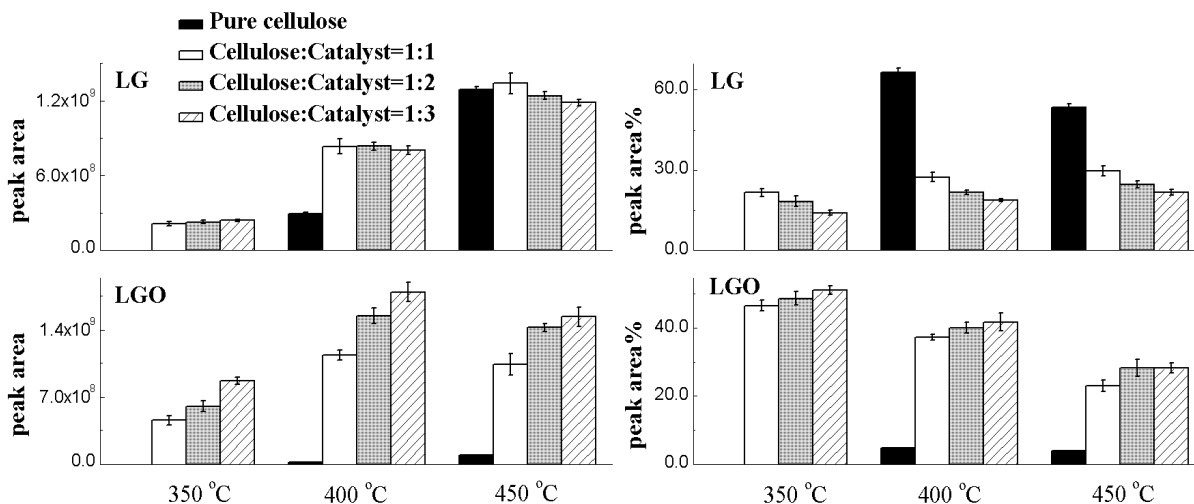


Fig. 6. Peak area and peak area% of the LG and LGO obtained at different cellulose/catalyst ratios

motionless during the analytical pyrolysis experiments. The contact between the cellulose and the catalyst was limited, and thus, the sufficient catalytic pyrolysis required high catalyst quantity. We might infer that during the industrial catalytic pyrolysis process, less catalyst should be required when the cellulose can be mixed and contacted well with the catalyst.

Effects of TiO₂ Type and Pyrolysis Time on the Product Distribution

Experiments were also performed to reveal the product distribution affected by the two crystal types of the TiO₂. Figure 7 shows the results of LGO obtained from using the two TiO₂ and two SO₄²⁻/TiO₂ catalysts, at the pyrolysis temperature of 400 °C, the cellulose/catalyst ratio of 1/2, and the pyrolysis time of 20 s. The results of the LG and other products are not shown in detail here. According to Fig. 7, the two SO₄²⁻/TiO₂ catalysts exhibited much better catalytic capability and selectivity to produce the LGO than the two TiO₂ catalysts. Moreover, the anatase TiO₂ performed better than the rutile TiO₂, while the SO₄²⁻/TiO₂ (anatase) also performed better than the SO₄²⁻/TiO₂ (rutile) catalyst.

The results further confirmed that the acidity of the catalysts was important relative to the LGO production, and the SO₄²⁻/TiO₂ (anatase) should be the best catalyst among the four catalysts tested in this study. Further studies are required to reveal the fundamental reason for the different catalytic capability caused by the TiO₂ type.

In addition, the analytical pyrolysis experiments were performed at three selected pyrolysis times (5 s, 10 s, and 20 s) to reveal the effects of pyrolysis time on the product distribution. The results indicated that the pyrolysis time did not have a great effect on the product composition (peak area% values), and only influenced the product yield (peak

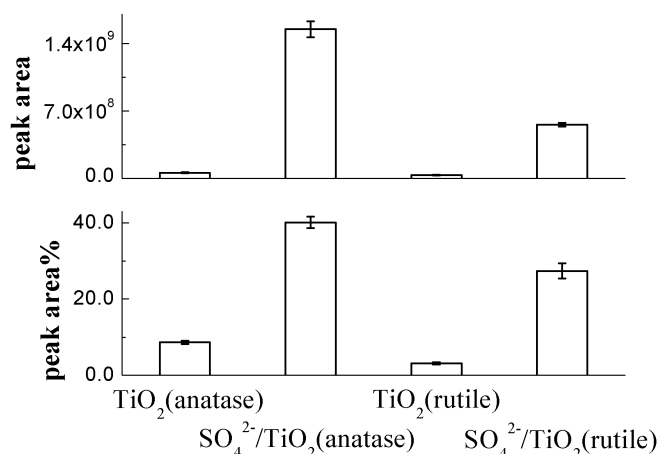


Fig. 7. Peak area and peak area% of LGO obtained from two TiO₂ and two SO₄²⁻/TiO₂ catalysts

area values) at 350 °C and 400 °C. Hence, the detailed results are not shown here. At 350 °C, the total product yield was increased when increasing the pyrolysis time from 5 s to 20 s. At 400 °C, the total product yield was increased when the pyrolysis time was prolonged from 5 s to 10 s, and almost kept constant afterwards. At 450 °C, the total product yield obtained at three different pyrolysis duration was similar. The results suggested that the complete decomposition of the cellulose could be shortened from 20 s to only 5 s by elevating pyrolysis temperature.

SO₄²⁻/TiO₂-catalyzed Conversion of LG

In addition to cellulose, pure LG was also used as a feedstock, mixed with the catalysts, and subjected to analytical fast pyrolysis. This series of experiments was to investigate the acid-catalyzed conversion of the LG with the following two purposes. First, the analytical pyrolysis experiments only employed a small amount of feedstock (0.30 mg cellulose). During the pyrolysis process, primary pyrolysis vapors would leave the reactor tube very quickly, without significant secondary cracking by the solid residues. However, this should not be the case in the large-scale pyrolysis reactor, and thus, it is necessary to investigate the secondary cracking of the primary pyrolysis vapors by the SO₄²⁻/TiO₂ catalyst.

As indicated above, the LG and LGO were the major products in the catalytic process. Hence, pure LG was employed and catalytically converted by the SO₄²⁻/TiO₂ under the same conditions as the cellulose, to reveal its secondary conversion characteristics. Second, this series of experiments were also able to confirm the catalytic capability and selectivity of the SO₄²⁻/TiO₂ catalyst on the LGO production.

During the non-catalytic process, pure LG was thermally stable, forming only a few cracking products during fast pyrolysis at 400 °C and 450 °C, with the typical total ion chromatogram shown in Fig. 3(d). By contrast, in the catalytic process, the LG was mainly converted to the LGO, together with some DGP, FF, and LAC as the by-products. The typical total ion chromatogram is shown in Fig. 3(e). The results clearly indicated that the SO₄²⁻/TiO₂ catalyst possessed good catalytic selectivity to promote the dehydration of LG to form the LGO. A possible mechanism for the LGO formation from acid-catalyzed decomposition of the LG was proposed by Halpern *et al.*, as shown in Fig. 8

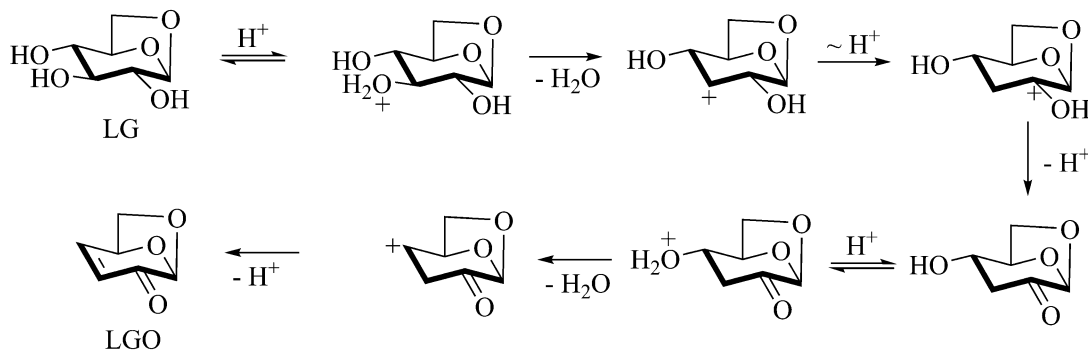


Fig. 8. The pathway for the acid-catalyzed conversion of LG to LGO

(Halpern *et al.* 1973). Based on these results, we might infer that during the large-scale pyrolysis reactor, moderate secondary cracking of the primary pyrolysis vapors could promote the conversion of the LG to LGO, facilitating the production of LGO with high yield and purity.

In addition, DGP was the most important by-product in the catalytic process. As a typical acid-catalyzed pyrolytic product, DGP was reported in several previous studies (Branca *et al.* 2010; Branca *et al.* 2011; Lu *et al.* 2011a). Shafizadeh *et al.* 1978 confirmed that the DGP would also tend to be converted to LGO in the acid-catalyzed process (H₃PO₄). However, due to the lack of the commercially available pure DGP, we are unable to determine whether the SO₄²⁻/TiO₂ could convert the DGP to LGO. Further studies will be performed when pure DGP is available.

CONCLUSIONS

1. Fast pyrolysis of cellulose mixed with the SO₄²⁻/TiO₂ catalysts offers a convenient way to produce LGO with high selectivity. During the catalytic process, the presence of the catalysts would inhibit the formation of the LG, significantly promote the LGO formation, and slightly increase the yields of DGP, FF, and LAC. The catalysts would also lower the temperature for the initial decomposition of cellulose to form organic volatile products.
2. Pyrolysis temperature played an important role on the LGO production. During the SO₄²⁻/TiO₂-catalyzed process, the highest LGO yield was obtained at the set pyrolysis temperature of 400 °C, and the highest LGO content was obtained at 350 °C with the peak area % over 50%.
3. The selectivity of the SO₄²⁻/TiO₂ catalyst on the LGO production would be promoted as changing the cellulose/catalyst ratio from 1/1 to 1/3. However, the pyrolysis time did not have much effect on the pyrolytic product composition.
4. Among the two TiO₂ and two SO₄²⁻/TiO₂ catalysts tested in this study, the SO₄²⁻/TiO₂ (anatase) performed best to produce LGO.
5. LG would be catalytically converted to LGO with high selectivity by the SO₄²⁻/TiO₂.

ACKNOWLEDGMENTS

The authors thank the National Natural Science Foundation of China (51106052), Program for New Century Excellent Talents in University (NCET-10-0374), National Key Technology R&D Program (2012BAD30B01), National High Technology R&D Program (2012AA051803), and Fundamental Research Funds for the Central Universities (11ZG08, 11QG25, 12ZP02) for financial support.

REFERENCES CITED

- Branca, C., Di Blasi, C., and Galgano, A. (2010). "Pyrolysis of corncobs catalyzed by zinc chloride for furfural production," *Ind. Eng. Chem. Res.* 49(20), 9743-9752.
- Branca, C., Galgano, A., Blasi, C., Esposito, M., and Di Blasi, C. (2011). "H₂SO₄-catalyzed pyrolysis of corncobs," *Energ Fuel* 25(1), 359-369.
- Bridgwater, A. V., and Peacocke, G. V. C. (2000). "Fast pyrolysis processes for biomass," *Renew. Sust. Energ. Rev.* 4(1), 1-73.
- Czernik, S., and Bridgwater, A. V. (2004). "Overview of applications of biomass fast pyrolysis oil," *Energ Fuel* 18(2), 590-598.
- Di Blasi, C., Branca, C., and Galgano, A. (2007). "Effects of diammonium phosphate on the yields and composition of products from wood pyrolysis," *Ind. Eng. Chem. Res.* 46(2), 430-438.
- Di Blasi, C., Branca, C., and Galgano, A. (2008). "Products and global weight loss rates of wood decomposition catalyzed by zinc chloride," *Energ Fuel* 22(1), 663-670.
- Dobele, G., Dizhbite, T., Rossinskaja, G., Telysheva, G., Meier, D., Radtke, S., and Faix, O. (2003). "Pre-treatment of biomass with phosphoric acid prior to fast pyrolysis: A promising method for obtaining 1,6-anhydrosaccharides in high yields," *J. Anal. Appl. Pyrol.* 68-69, 197-211.
- Dobele, G., Meier, D., Faix, O., Radtke, S., Rossinskaja, G., and Telysheva, G. (2001). "Volatile products of catalytic flash pyrolysis of celluloses," *J. Anal. Appl. Pyrol.* 58, 453-463.
- Dobele, G., Rossinskaja, G., Dizhbite, T., Telysheva, G., Meier, D., and Faix, O. (2005). "Application of catalysts for obtaining 1,6-anhydrosaccharides from cellulose and wood by fast pyrolysis," *J. Anal. Appl. Pyrol.* 74(1-2), 401-405.
- Fabbri, D., Torri, C., and Baravelli, V. (2007a). "Effect of zeolites and nanopowder metal oxides on the distribution of chiral anhydrosugars evolved from pyrolysis of cellulose: An analytical study," *J. Anal. Appl. Pyrol.* 80(1), 24-29.
- Fabbri, D., Torri, C., and Mancini, I. (2007b). "Pyrolysis of cellulose catalysed by nanopowder metal oxides: Production and characterisation of a chiral hydroxylactone and its role as building block," *Green Chem.* 9(12), 1374-1379.
- Fu, Q. R., Argyropoulos, D. S., Tilotta, D. C., and Lucia, L. A. (2008a). "Understanding the pyrolysis of CCA-treated wood Part I. Effect of metal ions," *J. Anal. Appl. Pyrol.* 81(1), 60-64.

- Fu, Q. R., Argyropoulos, D. S., Tilotta, D. C., and Lucia, L. A. (2008b). "Understanding the pyrolysis of CCA-treated wood. Part II. Effect of phosphoric acid," *J. Anal. Appl. Pyrol.* 82(1), 140-144.
- Guo, C., Yao, S., Cao, J., and Qian, Z. (1994). "Alkylation of isobutane with butenes over solid superacids, $\text{SO}_4^{2-}/\text{ZrO}_2$ and $\text{SO}_4^{2-}/\text{TiO}_2$," *Appl. Catal. A: Gen.* 107(2), 229-238.
- Halpern, Y., Riffer, R., and Broido, A. (1973). "Levoglucosenone (1,6-anhydro-3,4-dideoxy- β -D-pyranosen-2-one). A major product of the acid-catalyzed pyrolysis of cellulose and related carbohydrates," *J. Org. Chem.* 38, 204-209.
- Klampfl, C. W., Breuer, G., Schwarzingler, C., and Koll, B. (2006). "Investigations on the effect of metal ions on the products obtained from the pyrolysis of cellulose," *Acta Chim. Slov.* 53(4), 437-443.
- Lu, Q., Dong, C. Q., Zhang, X. M., Tian, H. Y., Yang, Y. P., and Zhu, X. F. (2011a). "Selective fast pyrolysis of biomass impregnated with ZnCl_2 to produce furfural: Analytical Py-GC/MS study," *J. Anal. Appl. Pyrol.* 90(2), 204-212.
- Lu, Q., Xiong, W. M., Li, W. Z., Guo, Q. X., and Zhu, X. F. (2009). "Catalytic pyrolysis of cellulose with sulfated metal oxides: A promising method for obtaining high yield of light furan compounds," *Bioresour. Technol.* 100(20), 4871-4876.
- Lu, Q., Yang, X. C., Dong, C. Q., Zhang, Z. F., Zhang, X. M., and Zhu, X. F. (2011b). "Influence of pyrolysis temperature and time on the cellulose fast pyrolysis products: Analytical Py-GC/MS study," *J. Anal. Appl. Pyrol.* 92(2), 430-438.
- Miftakhov, M. S., Valeev, F. A., and Gaisina, I. N. (1994). "Levoglucosenone: the properties, reactions, and use in fine organic synthesis," *Russ. Chem. Rev.* 63(10), 869-882.
- Mohan, D., Pittman, C. U., and Steele, P. H. (2006). "Pyrolysis of wood/biomass for bio-oil: A critical review," *Energ Fuel* 20(3), 848-889.
- Nowakowski, D. J., Woodbridge, C. R., and Jones, J. M. (2008). "Phosphorus catalysis in the pyrolysis behaviour of biomass," *J. Anal. Appl. Pyrol.* 83(2), 197-204.
- Ohnishi, A., Kato, K., and Takagi, E. (1975). "Curie-point pyrolysis of cellulose," *Polym. J.* 7(4), 431-437.
- Pappa, A., Mikedi, K., Tzamtzis, N., and Statheropoulos, M. (2006). "TG-MS analysis for studying the effects of fire retardants on the pyrolysis of pine-needles and their components," *J. Therm. Anal. Calorim.* 84(3), 655-661.
- Pattiya, A., Titiloye, J. O., and Bridgwater, A. V. (2008). "Fast pyrolysis of cassava rhizome in the presence of catalysts," *J. Anal. Appl. Pyrol.* 81(1), 72-79.
- Patwardhan, P. R., Satrio, J. A., Brown, R. C., and Shanks, B. H. (2009). "Product distribution from fast pyrolysis of glucose-based carbohydrates," *J. Anal. Appl. Pyrol.* 86(2), 323-330.
- Ponder, G. R., Richards, G. N., and Stevenson, T. T. (1992). "Influence of linkage position and orientation in pyrolysis of polysaccharides: A study of several glucans," *J. Anal. Appl. Pyrol.* 22(3), 217-229.
- Sarotti, A. M., Spanevello, R. A., and Suarez, A. G. (2007). "An efficient microwave-assisted green transformation of cellulose into levoglucosenone. Advantages of the use of an experimental design approach," *Green Chem.* 9(10), 1137-1140.
- Shafizadeh, F., Furneaux, R. H., and Stevenson, T. T. (1979). "Some reactions of levoglucosenone," *Carbohydr. Res.* 71(1), 1-352.

- Shafizadeh, F., Furneaux, R. H., Stevenson, T. T., and Cochran, T. G. (1978). "Acid-catalyzed pyrolytic synthesis and decomposition of 1,4:3,6-dianhydro- α -D-glucopyranose," *Carbohydr. Res.* 61, 519-528.
- Shen, D. K., and Gu, S. (2009). "The mechanism for thermal decomposition of cellulose and its main products," *Bioresour. Technol.* 100(24), 6496-6504.
- Shen, D. K., Xiao, R., Gu, S., and Luo, K. H. (2011). "The pyrolytic behavior of cellulose in lignocellulosic biomass: a review," *RSC Adv.* 1(9), 1641-1660.
- Sui, X. W., Wang, Z., Liao, B., Zhang, Y., and Guo, Q. X. (2012). "Preparation of levoglucosenone through sulfuric acid promoted pyrolysis of bagasse at low temperature," *Bioresour. Technol.* 103(1), 466-469.
- Torri, C., Lesci, I. G., and Fabbri, D. (2009). "Analytical study on the pyrolytic behaviour of cellulose in the presence of MCM-41 mesoporous materials," *J. Anal. Appl. Pyrol.* 85(1-2), 192-196.
- Wang, Z., Lu, Q., Zhu, X.-F., and Zhang, Y. (2011). "Catalytic fast pyrolysis of cellulose to prepare levoglucosenone using sulfated zirconia," *ChemSusChem* 4(1), 79-84.

Article submitted: January 23, 2012; Peer review completed: March 17, 2012; Revised version received and accepted: May 15, 2012; Published: May 17, 2012.